

Charged polariton luminescence from an organic semiconductor microcavity

Chiao-Yu Cheng, Hoyeon Kim and Noel C. Giebink[†]

*Department of Electrical Engineering, The Pennsylvania State University, University Park, PA,
16802 U.S.A.*

[†]email: ncg2@psu.edu

Abstract

Strong coupling light to polaron optical transitions in an organic semiconductor microcavity leads to an unusual class of polariton that possesses a net charge. This species may offer a range of technologically-useful optoelectronic properties but has thus far only been observed in passive reflectivity measurements. Here, we report room-temperature photoluminescence from both upper and lower branch polaron polariton states that originate from hole excitations in a p-doped 4,4'-cyclohexylidenebis[N,N-bis(4-methylphenyl)benzenamine] (TAPC) microcavity. Our observations under non-resonant excitation are in good agreement with classical dipole emission modeling, which suggests that polariton states in this system are populated radiatively via fluorescence from the polaron excited state reservoir. These results constitute one of the first observations of polaron luminescence from an organic semiconductor thin film and are an important prerequisite for realizing a charged polariton condensate.

Keywords: Polaron, strong coupling, cation, fluorescence

Light emission from microcavity polariton states is central to many of their most intriguing and technologically useful phenomena, including Bose-Einstein condensation, superfluidity, and polariton lasing¹⁻⁴. In organic semiconductor microcavities, neutral excitonic transitions typically provide the basis for strong coupling and result in polariton branches that are observable in both reflectivity and luminescence⁵. Recently, we used reflectivity measurements to demonstrate that radical ion transitions in a heavily doped organic semiconductor can also be strongly coupled to a cavity mode, resulting in charged polaritons that are thought to possess a range of unusual electric and magnetic properties⁶. While luminescence is commonly observed from trion polaritons in inorganic semiconductor systems⁷⁻¹⁰, emission from charged molecules is rare due to their large non-radiative decay rate¹¹⁻¹⁵ and thus it has been unclear whether luminescence can also be observed from organic charged polaritons.

Here, we report photoluminescence from the upper and lower polariton branches of a p-doped 4,4'-cyclohexylidenebis[N,N-bis(4-methylphenyl)benzenamine] (TAPC) planar microcavity under non-resonant excitation. Despite a low polaron photoluminescence quantum yield $\sim 10^{-4}$, agreement with classical dipole emission modeling over a wide range of cavity detuning leads us to conclude that polariton states are populated primarily via fluorescence from the polaron excited state reservoir. These results clarify the manner in which charged polariton states are populated and are an important step toward possible lasing or condensation phenomena with this species in the future.

Figure 1a shows a schematic of the microcavity structure together with an energy level diagram illustrating the manner in which TAPC is p-doped by MoO₃ through ground-state electron transfer from the highest occupied molecular orbital (HOMO). This results in two new optical transitions, P₁ and P₂, that respectively correspond to excitation of an electron into, and

out of, the now partially-occupied HOMO¹⁵. Though the cartoon in Fig. 1a is drawn for an isolated molecular cation, these optical transitions remain largely unchanged in the solid state due weak intermolecular electronic coupling, where P₁ is now equivalently viewed as the excitation of a hole polaron.

Figure 1b shows the absorption spectrum measured for a 10 wt% MoO₃:TAPC film. There, the P₁ hole transition peaks at $E_p = 1.77$ eV, with the shoulder at ~ 2.2 eV also originating from a hole transition to another, slightly deeper molecular orbital; the P₂ and neutral molecule transitions both take place at higher energy (~ 3.3 eV and ~ 4 eV, respectively⁶) and are not captured on this axis. Based on the absorption cross-section measured for TAPC⁺ in solution ($\sigma = 2.5 \times 10^{-16}$ cm²),⁶ the polaron density in the film is estimated to be $\sim 6 \times 10^{19}$ cm⁻³. Figure 1b also shows the photoluminescence (PL) spectrum of this film (blue line), acquired alongside that of an undoped reference TAPC film (green line) under $\lambda = 375$ nm excitation using a $\lambda = 410$ nm long-pass filter. Relative to the reference PL, neutral TAPC fluorescence in the doped film is blue-shifted and strongly quenched. Quenching presumably reflects energy transfer to the lower energy polaron transitions whereas the blue-shift is a consequence of the broad density of states (DOS) in the film, since molecules in the upper portion of the DOS (i.e. those with the highest HOMOs and thus more likely to possess a lower HOMO-LUMO gap) are the most likely to be ionized by MoO₃ (and occupied by extrinsic holes), effectively eliminating them from the neutral molecule fluorescence ensemble¹⁵.

The most striking feature of the doped film PL spectrum, however, is the weak emission band located at 1.66 eV (see inset of Fig. 1b), which we assign to the P₁ polaron transition. Emission from charged molecules is rare in the literature due to fast internal conversion¹¹⁻¹⁵ and all the more remarkable in this case because it is observed in the solid state at room temperature.

It is observed here under non-resonant ($\lambda = 375$ nm; green line) and near-resonant ($\lambda = 633$ nm, orange line) excitation, though in the latter case, a sharp additional line at ~ 1.77 eV is superimposed. This is a Raman line of the TAPC cation, an assignment supported by the fact that it shifts appropriately upon exciting at $\lambda = 640$ nm (red line) while the polaron emission remains unchanged. High resolution Raman spectroscopy shows that this peak is actually a doublet, with Raman shifts of 1580 cm^{-1} and 1601 cm^{-1} that originate from neutral TAPC but gain strongly in intensity for TAPC⁺.

Figure 1c shows that the polaron PL is photostable when excited at $\lambda = 640$ nm but degrades rapidly when excited at $\lambda = 375$ nm. The PL degradation in the latter case is irreversible, is largely the same regardless of whether the measurement is carried out in ambient air or vacuum, and is mirrored by a reduction in the polaron absorbance. These observations suggest that TAPC molecular cations may undergo chemical degradation in the presence of neutral TAPC excitons, possibly via the same exciton-polaron annihilation mechanism that causes molecular fragmentation in organic light emitting diodes^{16,17}. Alternatively, it may be that directly exciting the P2 transition of TAPC⁺ (which also absorbs at $\lambda = 375$ nm)⁶ leads to molecular instability.

The comparable intensities of the Raman and polaron PL spectra in Fig. 1b attest to the very low PL quantum yield of the latter, which we estimate to be $\phi_0 \sim 10^{-4}$ using a film of tris-(8-hydroxyquinoline)aluminum (Alq₃) as a reference standard¹⁸. This is consistent with the rapid, $\tau_0 \sim 1$ ps decay of the polaron excited state measured via ultrafast transient absorption⁶ and implies radiative and non-radiative polaron decay rates of $k_r = \phi_0/\tau_0 \sim 10^8\text{ s}^{-1}$ and $k_{nr} \approx 1/\tau_0 \sim 10^{12}\text{ s}^{-1}$, respectively. The radiative rate is in good agreement with that predicted by the Strickler-Berg relation on the basis of the polaron molar absorption coefficient^{6,15}.

Figure 2a shows the angle-dependent reflectivity spectra collected for the cavity architecture illustrated in Fig. 1a, where the thickness of the 10 wt% MoO₃:TAPC active layer is chosen to negatively detune the cavity mode (energy E_C at zero in-plane wavevector) relative to the polaron transition by $\Delta = E_C - E_P = -0.11$ eV. Consistent with previous work⁶, we observe a clear anti-crossing in the reflectivity dips about the bare polaron transition energy (denoted by the green dashed line) that signifies the existence of upper and lower polariton (UP and LP, respectively) branches in the strong coupling regime. A similar evolution is observed in angle-dependent PL spectra collected from the cavity under non-resonant ($\lambda = 375$ nm, with periodic translations to avoid photodegradation) excitation in Figure 2b. There, emission from the LP branch dominates the spectrum at low angle whereas emission from the UP branch dominates at high angle. Figure 2c plots the polariton mode dispersions determined from Gaussian multi-peak fitting of the reflectivity and PL data, demonstrating good overall agreement between the two. The data are well-described using a simple coupled oscillator model shown by the solid red lines, which yields a vacuum Rabi splitting of $\hbar\Omega = 0.11 \pm 0.03$ eV based on a cavity mode linewidth, $\delta_\gamma \sim 0.08$ eV, and negligible homogeneous broadening of the polaron transition^{19,20}.

Figure 3a displays a map of the PL intensity for this cavity (not normalized at each individual angle as in Fig. 2b), which demonstrates that the emission peaks in the LP branch at zero in-plane wavevector ($k_{||} = 0$), similar to neutral organic polariton systems^{5,21}. By contrast, decreasing the MoO₃:TAPC layer thickness to positively detune the cavity ($\Delta = +0.11$ eV) leads to a relative increase in UP emission intensity as shown in Fig. 3b. This may simply reflect an increasing contribution of background fluorescence into the UP mode²¹⁻²⁴ that originates from the neutral TAPC emission tail (see Fig. 1b); filtering of this fluorescence tail through the UP mode may also explain the systematic offset between the upper branch PL dispersion and

reflectivity data²⁵. Relaxation from the upper to lower branch is inefficient because the predominantly photonic character of the UP branch suppresses the interbranch relaxation rate, which is proportional to the product of UP and LP polaronic Hopfield coefficients^{5,24,26}. Combined with the faster radiative decay of the more photon-like UP (roughly equal to the cavity photon lifetime, $\tau_c \sim 8$ fs), which affords less time to relax in the first place, the increase in UP emission observed for the positively detuned cavity is not unexpected.

Figure 3c and 3d show that transfer matrix dipole emission modeling qualitatively reproduces the photoluminescence of each cavity, suggesting that the PL in both cases can be understood on the basis of reservoir excited state fluorescence into the polariton modes. This radiative mode of polariton population is associated with emission from uncoupled polaron (and neutral TAPC tail) excited states into the wedge of optical étendue that makes up the photonic component of a polariton mode^{22,23}. The agreement between data and simulation in Fig. 3 not only argues for a predominantly radiative mode of polariton population (as opposed to phonon scattering from the polaron excited state reservoir)^{27–29}, it also implies that inter- and intra-branch polariton relaxation are negligible since they are not accounted for in the model.

Figure 4a examines the integrated LP emission intensity collected at normal incidence as a function of the cavity detuning. The data are corrected for changes in the absorbed fraction of the $\lambda = 375$ nm pump laser and are normalized to the emission from a bare 10% MoO₃:TAPC film on Si measured under identical conditions. This plot shows that the relative LP emission yield peaks when the detuning equals the Stokes shift of the uncoupled PL (roughly 0.11 eV), in reasonable quantitative agreement with the transfer matrix model (solid line) except at large negative detuning, where the uncertainty in the experimental data increases due to a higher order cavity mode that strongly increases the pump absorption. These observations lend further support

to the notion that LP states are populated radiatively in proportion to their overlap with the bare polaron fluorescence spectrum (i.e. the polaron excited state reservoir) as illustrated in Fig. 4b. The apparent lack of competitive phonon scattering into the LP branch in this case may be related to the high energy of the dominant polaron Raman modes (~ 0.2 eV; see Fig. 1b) which, combined with the large Stokes shift, would require a cavity detuning of almost $\Delta = -0.35$ eV (and thus a very photon-like LP branch) to satisfy energy conservation in a transition to $k_{\parallel} = 0$.

It remains to be seen whether the formation of a charged polariton condensate is feasible in this system under realistic experimental conditions. While the ultrafast polaron excited state lifetime is not conducive to large reservoir populations, it may still be possible to reach the stimulated scattering regime if impulsive (e.g. ~ 100 fs) excitation pulses are used, resonant phonon scattering can be exploited to populate the LP branch more efficiently, and the cavity Q is increased to boost the polariton lifetime^{30,31}. By contrast, the \sim ps polaron excited state lifetime is not expected to be detrimental for resonantly-excited phenomena such as polariton parametric scattering^{32,33} and superfluidity³ since the polariton lifetime is still likely to be dominated by that of the cavity photon for $Q < 1000$. Charged polaritons may prove particularly useful for studying these types of phenomena given their potential for enhanced polariton-polariton interaction as well as the ability to induce trapping potentials by electrically gating the local polaron density⁶.

In summary, we have identified the first instance of polaron luminescence in solid-state organic semiconductors and have demonstrated both upper and lower branch polariton luminescence from this species in the strong coupling regime. The quantum yield of polaron luminescence is low ($\sim 10^{-4}$) owing to fast internal conversion, yet the predominant mode of polariton population still appears to be radiative via fluorescence from the polaron excited state

reservoir. Our central finding that charged polariton luminescence can be observed from an organic semiconductor microcavity not only represents an important development for the future study of this species but also marks a key step toward the realization of a charged polariton condensate.

Methods

Modeling: Reflectivity was modeled using the transfer matrix method based on thicknesses and optical constant dispersions determined via variable angle spectroscopic ellipsometry for each material. Polariton dispersion relations obtained from reflectivity were modeled using the coupled oscillator Hamiltonian described in Ref. [6]. Dipole emission modeling was carried out using the method of source terms³⁴ with the bare film PL serving as the source spectrum.

Fabrication: Deposition was carried out in a vacuum thermal evaporator with a base pressure of 4×10^{-7} Torr using TAPC that was purified once via gradient sublimation. Cavity samples were deposited on Si substrates whereas bare reference samples were deposited on glass cover slides and Si substrates for absorption and photoluminescence measurements, respectively.

Characterization: Angle-dependent reflectivity was measured by mounting samples on a motorized rotation stage and using collimated light from a laser-driven Xe lamp, filtered through a monochromator and polarized with a wire grid polarizer. Photoluminescence was acquired through a lens with a collection half angle of $\sim 4^\circ$ and analyzed through a polarizer using a spectrograph with a cooled Si CCD detector. Continuous wave lasers ($\lambda = 375, 640$ nm) were used for excitation with intensities of approximately 400 mW cm^{-2} . Samples were measured in air without encapsulation and were translated periodically to avoid photodegradation effects when exciting with $\lambda = 375$ nm light.

Acknowledgements: This work was supported by the National Science Foundation under Grant No. DMR-1654077.

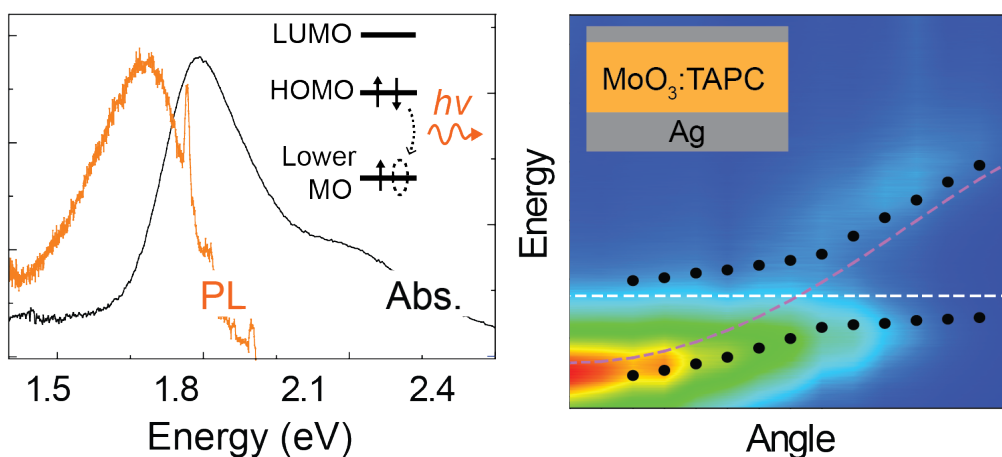
References

- (1) Fraser, M. D.; Höfling, S.; Yamamoto, Y. Physics and Applications of Exciton–Polariton Lasers. *Nat. Mater.* **2016**, *15*, 1049–1052.
- (2) Amo, A.; Lefrère, J.; Pigeon, S.; Adrados, C.; Ciuti, C.; Carusotto, I.; Houdré, R.; Giacobino, E.; Bramati, A. Superfluidity of Polaritons in Semiconductor Microcavities. *Nat. Phys.* **2009**, *5*, 805–810.
- (3) Lerario, G.; Fieramosca, A.; Barachati, F.; Ballarini, D.; Daskalakis, K. S.; Dominici, L.; Giorgi, M. D.; Maier, S. A.; Gigli, G.; Kéna-Cohen, S.; et al. Room-Temperature Superfluidity in a Polariton Condensate. *Nat. Phys.* **2017**, *13*, 837–841.
- (4) Byrnes, T.; Kim, N. Y.; Yamamoto, Y. Exciton–Polariton Condensates. *Nat. Phys.* **2014**, *10*, 803–813.
- (5) Holmes, R. J.; Forrest, S. R. Strong Exciton–Photon Coupling in Organic Materials. *Org. Electron.* **2007**, *8*, 77–93.
- (6) Cheng, C.-Y.; Dhanker, R.; Gray, C. L.; Mukhopadhyay, S.; Kennehan, E. R.; Asbury, J. B.; Sokolov, A.; Giebink, N. C. Charged Polaron Polaritons in an Organic Semiconductor Microcavity. *Phys. Rev. Lett.* **2018**, *120*, 017402.
- (7) Dhara, S.; Chakraborty, C.; Goodfellow, K. M.; Qiu, L.; O’Loughlin, T. A.; Wicks, G. W.; Bhattacharjee, S.; Vamivakas, A. N. Anomalous Dispersion of Microcavity Trion-Polaritons. *Nat. Phys.* **2018**, *14*, 130–133.
- (8) Möhl, C.; Graf, A.; Berger, F. J.; Lüttgens, J.; Zakharko, Y.; Lumsargis, V.; Gather, M. C.; Zaumseil, J. Trion-Polariton Formation in Single-Walled Carbon Nanotube Microcavities. *ACS Photonics* **2018**, *5*, 2074–2080.
- (9) Rapaport, R.; Harel, R.; Cohen, E.; Ron, A.; Linder, E.; Pfeiffer, L. N. Negatively Charged Quantum Well Polaritons in a GaAs/AlAs Microcavity: An Analog of Atoms in a Cavity. *Phys. Rev. Lett.* **2000**, *84*, 1607–1610.
- (10) Cuadra, J.; Baranov, D. G.; Wersäll, M.; Verre, R.; Antosiewicz, T. J.; Shegai, T. Observation of Tunable Charged Exciton Polaritons in Hybrid Monolayer WS₂–Plasmonic Nanoantenna System. *Nano Lett.* **2018**, *18*, 1777–1785.
- (11) Zimmer, K.; Hoppmeier, M.; Schweig, A. Fluorescence of an Organic Radical Cation (5,10-Dihydro-5,10-Dimethylphenazine^{•+}) in Liquid Solution at Room Temperature. *Chem. Phys. Lett.* **1998**, *293*, 366–370.
- (12) Brodard, P.; Sarbach, A.; Gumy, J.-C.; Bally, T.; Vauthey, E. Excited-State Dynamics of Organic Radical Ions in Liquids and in Low-Temperature Matrices. *J. Phys. Chem. A* **2001**, *105*, 6594–6601.
- (13) Zimmer, K.; Gödicke, B.; Hoppmeier, M.; Meyer, H.; Schweig, A. Fluorescence Spectroscopic Studies on the Radical Cations of Tetrathiafulvalenes. *Chem. Phys.* **1999**, *248*, 263–271.

- (14) Fujitsuka, M.; Majima, T. Reaction Dynamics of Excited Radical Ions Revealed by Femtosecond Laser Flash Photolysis. *J. Photochem. Photobiol. C Photochem. Rev.* **2018**, *35*, 25–37.
- (15) The Electronic Structure of Organic Semiconductors. In *Electronic Processes in Organic Semiconductors*; Wiley-Blackwell, 2015; pp 1–86.
- (16) Giebink, N. C.; D'Andrade, B. W.; Weaver, M. S.; Mackenzie, P. B.; Brown, J. J.; Thompson, M. E.; Forrest, S. R. Intrinsic Luminance Loss in Phosphorescent Small-Molecule Organic Light Emitting Devices Due to Bimolecular Annihilation Reactions. *J. Appl. Phys.* **2008**, *103*, 044509.
- (17) Giebink, N. C.; D'Andrade, B. W.; Weaver, M. S.; Brown, J. J.; Forrest, S. R. Direct Evidence for Degradation of Polaron Excited States in Organic Light Emitting Diodes. *J. Appl. Phys.* **2009**, *105*, 124514.
- (18) Kawamura, Y.; Sasabe, H.; Adachi, C. Simple Accurate System for Measuring Absolute Photoluminescence Quantum Efficiency in Organic Solid-State Thin Films. *Jpn. J. Appl. Phys.* **2004**, *43*, 7729.
- (19) Houdré, R.; Stanley, R. P.; Ilegems, M. Vacuum-Field Rabi Splitting in the Presence of Inhomogeneous Broadening: Resolution of a Homogeneous Linewidth in an Inhomogeneously Broadened System. *Phys. Rev. A* **1996**, *53*, 2711–2715.
- (20) Tropsch, L.; Dietrich, C. P.; Herbst, S.; Kanibolotsky, A. L.; Skabara, P. J.; Würthner, F.; Samuel, I. D. W.; Gather, M. C.; Höfling, S. Influence of Optical Material Properties on Strong Coupling in Organic Semiconductor Based Microcavities. *Appl. Phys. Lett.* **2017**, *110*, 153302.
- (21) Lidzey, D. G.; Fox, A. M.; Rahn, M. D.; Skolnick, M. S.; Agranovich, V. M.; Walker, S. Experimental Study of Light Emission from Strongly Coupled Organic Semiconductor Microcavities Following Nonresonant Laser Excitation. *Phys. Rev. B* **2002**, *65*, 195312.
- (22) Michetti, P.; La Rocca, G. C. Simulation of J-Aggregate Microcavity Photoluminescence. *Phys. Rev. B* **2008**, *77*, 195301.
- (23) Michetti, P.; La Rocca, G. C. Exciton-Phonon Scattering and Photoexcitation Dynamics in J-Aggregate Microcavities. *Phys. Rev. B* **2009**, *79*, 035325.
- (24) Lodden, G. H.; Holmes, R. J. Electrical Excitation of Microcavity Polaritons by Radiative Pumping from a Weakly Coupled Organic Semiconductor. *Phys. Rev. B* **2010**, *82*, 125317.
- (25) Tischler, J. R.; Bradley, M. S.; Bulović, V.; Song, J. H.; Nurmikko, A. Strong Coupling in a Microcavity LED. *Phys. Rev. Lett.* **2005**, *95*, 036401.
- (26) Grant, R. T.; Michetti, P.; Musser, A. J.; Gregoire, P.; Virgili, T.; Vella, E.; Cavazzini, M.; Georgiou, K.; Galeotti, F.; Clark, C.; et al. Efficient Radiative Pumping of Polaritons in a Strongly Coupled Microcavity by a Fluorescent Molecular Dye. *Adv. Opt. Mater.* **2016**, *4*, 1615–1623.
- (27) Litinskaya, M.; Reineker, P.; Agranovich, V. M. Fast Polariton Relaxation in Strongly Coupled Organic Microcavities. *J. Lumin.* **2004**, *110*, 364–372.
- (28) Somaschi, N.; Mouchliadis, L.; Coles, D.; Perakis, I. E.; Lidzey, D. G.; Lagoudakis, P. G.; Savvidis, P. G. Ultrafast Polariton Population Build-up Mediated by Molecular Phonons in Organic Microcavities. *Appl. Phys. Lett.* **2011**, *99*, 143303.
- (29) Coles, D. M.; Michetti, P.; Clark, C.; Tsoi, W. C.; Adawi, A. M.; Kim, J.-S.; Lidzey, D. G. Vibrationally Assisted Polariton-Relaxation Processes in Strongly Coupled Organic-Semiconductor Microcavities. *Adv. Funct. Mater.* **2011**, *21*, 3691–3696.
- (30) Carusotto, I.; Ciuti, C. Quantum Fluids of Light. *Rev. Mod. Phys.* **2013**, *85*, 299–366.

- (31) Daskalakis, K. S.; Maier, S. A.; Murray, R.; Kéna-Cohen, S. Nonlinear Interactions in an Organic Polariton Condensate. *Nat. Mater.* **2014**, *13*, 271–278.
- (32) Savvidis, P. G.; Baumberg, J. J.; Stevenson, R. M.; Skolnick, M. S.; Whittaker, D. M.; Roberts, J. S. Angle-Resonant Stimulated Polariton Amplifier. *Phys. Rev. Lett.* **2000**, *84*, 1547–1550.
- (33) Tartakovskii, A. I.; Skolnick, M. S.; Krizhanovskii, D. N.; Kulakovskii, V. D.; Stevenson, R. M.; Butté, R.; Baumberg, J. J.; Whittaker, D. M.; Roberts, J. S. Stimulated Polariton Scattering in Semiconductor Microcavities: New Physics and Potential Applications. *Adv. Mater.* **2001**, *13*, 1725–1730.
- (34) Benisty, H.; Stanley, R.; Mayer, M. Method of Source Terms for Dipole Emission Modification in Modes of Arbitrary Planar Structures. *JOSA A* **1998**, *15*, 1192–1201.

TOC Figure



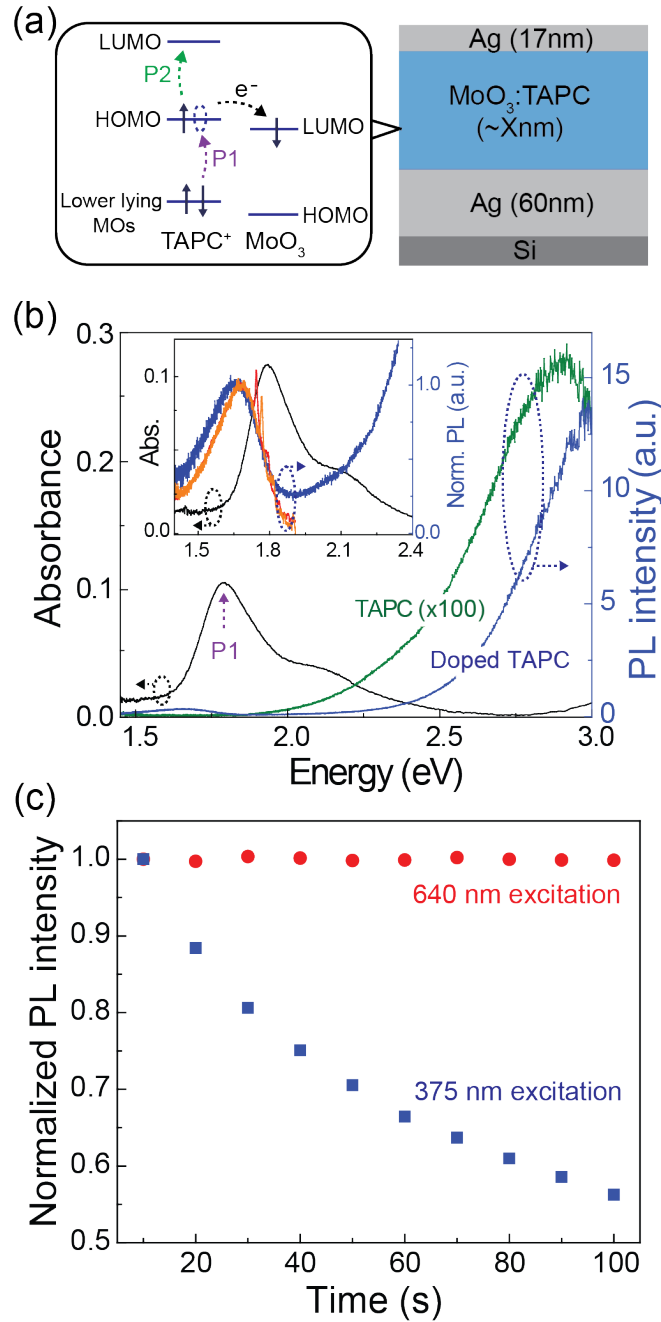


Figure 1. (a) Schematic showing the microcavity structure and polaron optical transitions that arise upon p-doping TAPC with MoO₃. The thickness of the MoO₃:TAPC layer in the cavity ranges from 175 nm to 145 nm depending on its detuning. (b) Absorption (left-hand axis) and emission (right-hand axis) spectra collected from 50 nm-thick film of neat TAPC and a 165 nm-thick film of 10 wt% MoO₃:TAPC under $\lambda = 375$ nm excitation; the inset shows a magnified

view of these spectra in the vicinity of the P_1 polaron transition. Photoluminescence spectra excited at $\lambda = 633$ nm (orange line) and $\lambda = 640$ nm (red line) exhibit a sharp peak at ~ 1.77 eV that originates from the 1580 cm^{-1} Raman shift of TAPC^+ . (c) The polaron emission is photostable under $\lambda = 640$ nm (red circles) excitation but degrades rapidly and irreversibly when excited by $\lambda = 375$ nm (blue squares) light with the same intensity.

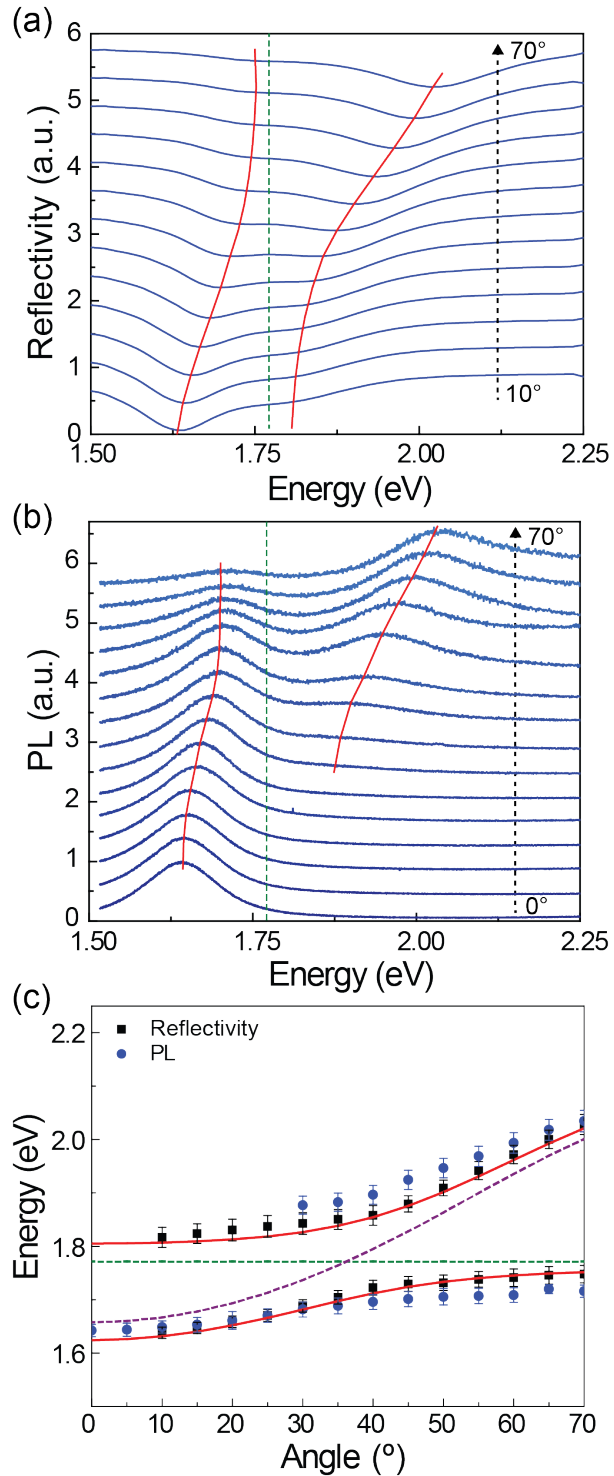


Figure 2. (a) S-polarized reflectivity spectra collected from a 165 nm-thick 10 wt% MoO₃:TAPC microcavity ($\Delta = -0.11$ eV) at incidence angles ranging from 10° to 70° in 5° increments. (b) Normalized photoluminescence spectra collected from the same sample, exciting

non-resonantly at $\lambda = 375$ nm and detecting through an s-oriented polarizer at angles ranging from 0° to 70° . The spectra in both panels are offset vertically for clarity, with dashed green lines denoting the bare polaron transition energy and red lines drawn as a guide to the eye. **(c)** Polariton dispersion extracted via Gaussian peak fitting of the reflectivity (black squares) and emission (blue circles) spectra in panels (a) and (b). Red lines result from fitting the reflectivity data with a coupled oscillator model based on the bare cavity mode dispersion and polaron transition energy shown by the dashed purple and green lines, respectively.

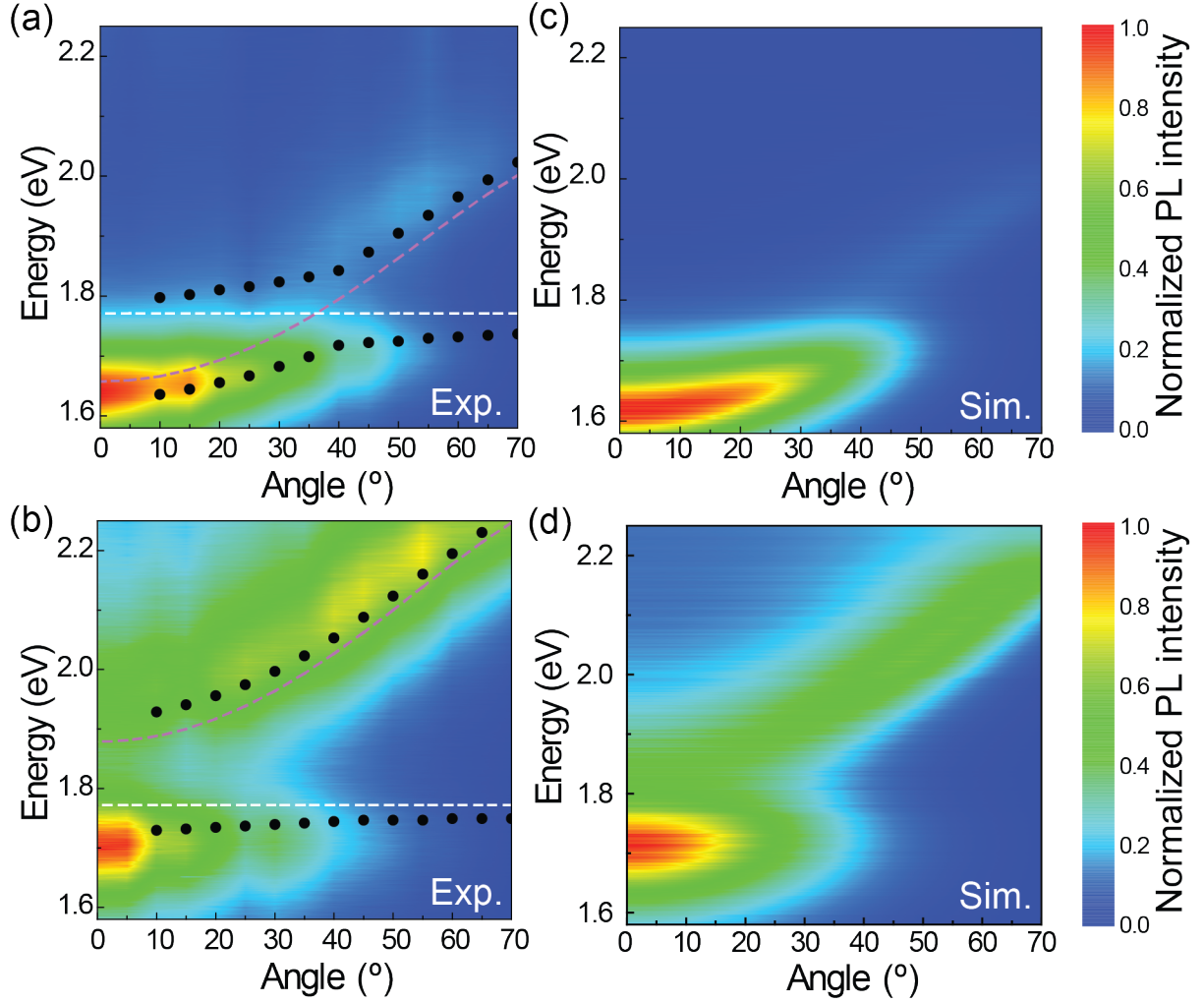


Figure 3. False color map of the angle-resolved, s-polarized photoluminescence intensity collected from **(a)** a negatively-detuned cavity ($\Delta = -0.11$ eV) and **(b)** a positively-detuned cavity ($\Delta = +0.11$ eV) under non-resonant, $\lambda = 375$ nm excitation. Solid black circles denote the dispersion observed in reflectivity and purple and white dashed lines indicate the uncoupled cavity mode dispersion and polaron transition energy, respectively. The s-polarized photoluminescence intensity simulated for each cavity via transfer matrix dipole emission modeling is shown in **(c)** and **(d)**, respectively.

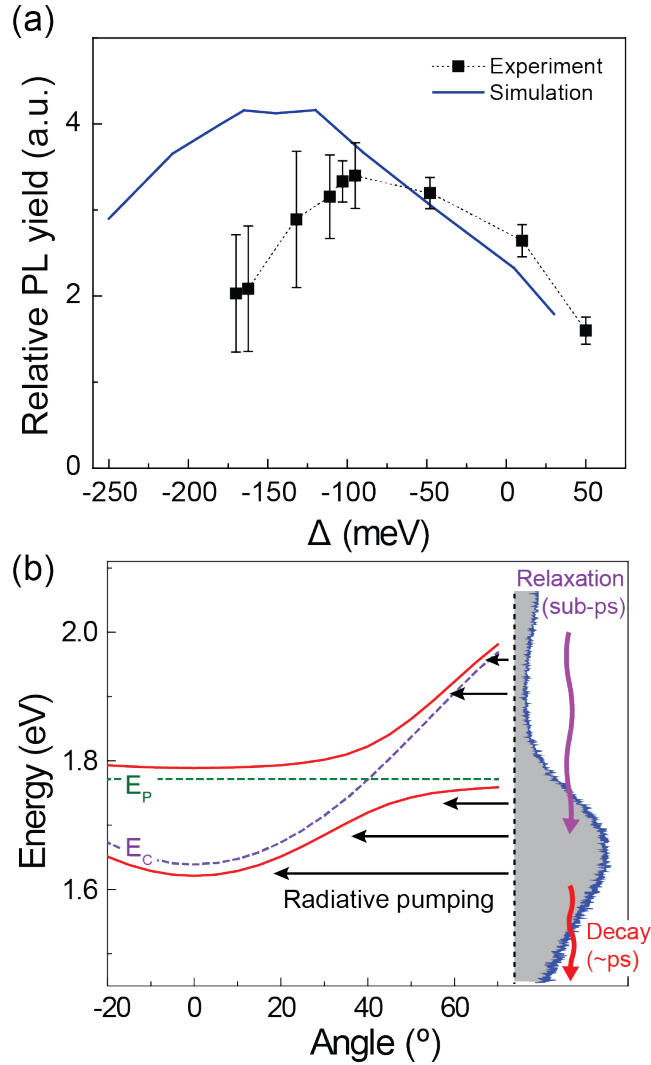


Figure 4. (a) Relative intensity of LP emission collected at normal incidence for a series of samples with different cavity detuning. The data are corrected for changes in the absorbed fraction of the $\lambda = 375$ nm pump laser and are normalized to the emission intensity from a bare film on Si measured under identical conditions. (b) Schematic showing the dominant polariton population and relaxation pathways in this system. Fast vibronic relaxation following non-resonant excitation (purple arrow) leads to a reservoir of polaron excited states with a distribution approximated by the bare polaron photoluminescence spectrum shown in gray (note that the high energy component above ~ 1.9 eV is the neutral TAPC emission tail). These

reservoir states decay on a \sim ps timescale (red arrow) and populate the lower polariton branch mainly via radiative pumping. Dashed green, dashed purple, and solid red lines correspond to the bare polaron transition energy, cavity mode dispersion, and polariton dispersion of the $\Delta = -0.13$ eV sample in (a).